

Primljen / Received: 2.11.2020.

Ispravljen / Corrected: 30.8.2021.

Prihvaćen / Accepted: 26.11.2021.

Dostupno online / Available online: 10.1.2022.

# Effect of steel fibres on reinforced concrete beam-column joints under reversed cyclic loading

## Authors:



Assoc.Prof. **Recep Kadir Pekgökgöz**, PhD. CE  
Harran University, Turkey  
Faculty of technical studies  
Civil Engineering Department  
[recepkadir@harran.edu.tr](mailto:recepkadir@harran.edu.tr)



Assist.Prof. **Fatih Avcil**, PhD. CE  
Bitlis Eren University, Turkey  
Faculty of technical studies  
[favcil@beu.edu.tr](mailto:favcil@beu.edu.tr)

**Corresponding author**

Research Paper

**Recep Kadir Pekgökgöz, Fatih Avcil**

## Effect of steel fibres on reinforced concrete beam-column joints under reversed cyclic loading

The vibrations produced by earthquakes cause large horizontal forces in beam-column joints. If these forces exceed the limit values that the joints can withstand, severe irreparable damage might occur. Experimental and analytical studies were conducted to determine the energy dissipation capacity and ductility of beam-column joints by using the Self-Compacting Concrete (SCC) and Normal Concrete (NC) mixes containing various quantities of steel fibres. Test results were compared with the results obtained using the test specimen made of normal concrete. The test results reveal similar behaviour of normal concrete and self-compacting concrete with regard to energy dissipation capacity. The use of steel fibres is known to increase ductility. This study shows that this behaviour is more prominent in the case of 1 % fibre volume ratio.

### Key words:

cyclic loading, steel fibre, energy dissipation, self-compacting concrete, ductility

Prethodno priopćenje

**Recep Kadir Pekgökgöz, Fatih Avcil**

## Utjecaj čeličnih vlakana na armiranobetonski spoj grede i stupa pri cikličnom opterećenju

Vibracije izazvane potresom uzrokuju snažne horizontalne sile u spojevima greda i stupova. Ako su granične vrijednosti opterećenja premašene, dolazi do nepopravljivih oštećenja. Provedena su eksperimentalna i analitička istraživanja kako bi se odredio kapacitet disipacije energije i duktilnost spojeva greda i stupova, a u tu su svrhu korištene mješavine samozbijajućeg betona i običnog betona kojima su dodavane različite količine čeličnih vlakana. Rezultati ispitivanja uspoređeni su s rezultatima koji su dobiveni na uzorcima običnog betona. Rezultati dobiveni ispitivanjem pokazuju da se obični beton i samozbijajući beton slično ponašaju u pogledu kapaciteta disipacije energije. Poznato je da čelična vlakna povećavaju duktilnost. U ovom je radu utvrđeno da je duktilnost najizraženija pri volumnom udjelu vlakana od 1 %.

### Ključne riječi:

ciklično opterećenje, čelična vlakna, disipacija energije, samozbijajući beton, duktilnost

### 1. Introduction

The beam-column joint is of great importance in designing moment resisting frame structures. The provision of strength and ductility depends on proper detailing of the column beam joints. Many studies have been carried out in current literature to determine behaviour of a normal concrete beam-column joint [1-5]. As a result of these studies on the production and use of fibre reinforced composites, it was established that steel fibre is capable of improving specimen behaviour especially with regard to the energy dissipation capacity and ductility [6]. However, very little research has been made on the behaviour of concrete beam-column joints with fibre reinforcement, especially under seismic loading [7-9]. Fibre reinforcement is an excellent alternative material for enhancing mechanical response of beam-column joints. Fibres used in concrete structures increase the ductility, energy absorption capacity, flexural strength, and tensile strength [10, 11].

Some investigations have been made to determine how fibre reinforcement affects durability and ductility. Studies by Oh [12] and Para-Montesinos and Wight [13] show that steel fibre reinforcement significantly increases flexural strength of structures. It has also been established that the steel fibre-reinforced concrete beam-column joint remarkably increases the shear strength and deformation capacity [14, 15]. To improve behaviour of the low strength reinforced concrete structures under earthquake load, high-performance fibre reinforced cement composites (HPFRCC) with thicknesses ranging from 20-50 mm have been studied for the production of prefabricated plaques [16]. Yurdakul and Avşar [17] report that the reinforced concrete beam-column connection repaired

with the carbon fibre-reinforced polymer is pretty effective in terms of strength and energy dissipation capacity. Experimental studies have been carried out to determine how the variation of steel fibre content in concrete mix affects the anchorage capacity and ductility on the beam-column joint of high-strength concrete [18]. The results of the study show that the anchorage capacity and ductility of the joint increase with an increase of steel fibre proportion in the concrete mix. Also, some researchers have investigated steel fibre reinforcement as an alternative way for reducing proportion of stirrups in beam-column joints [19].

### 2. Research objective

This experimental study presents various types of full-scale concrete beam-column joints reinforced with various amounts of steel fibres subjected to reversed cyclic loading. Normal Concrete (NC) and Self-Compacting Concrete (SCC) mixes were produced for this purpose, with the percentage of steel fibres by volume of concrete amounting to 0 %, 0.5 %, and 1.0 %. The design of the beam-column concrete and joint region for each specimen was made according to "Turkish requirements for design and construction of reinforced concrete structures" [20]. Even though full-sized normal concrete research has already been reported in the literature, there are no self-compacting concrete studies containing varying amounts of steel fibres.

Figure 1 shows details of test specimens of the reinforced concrete beam-column connection. Concrete cover is taken to be 30 mm in beam sections and 25 mm in column sections. Stirrups were placed in all regions except in the column-beam joint area. They were not placed in the column-beam joint

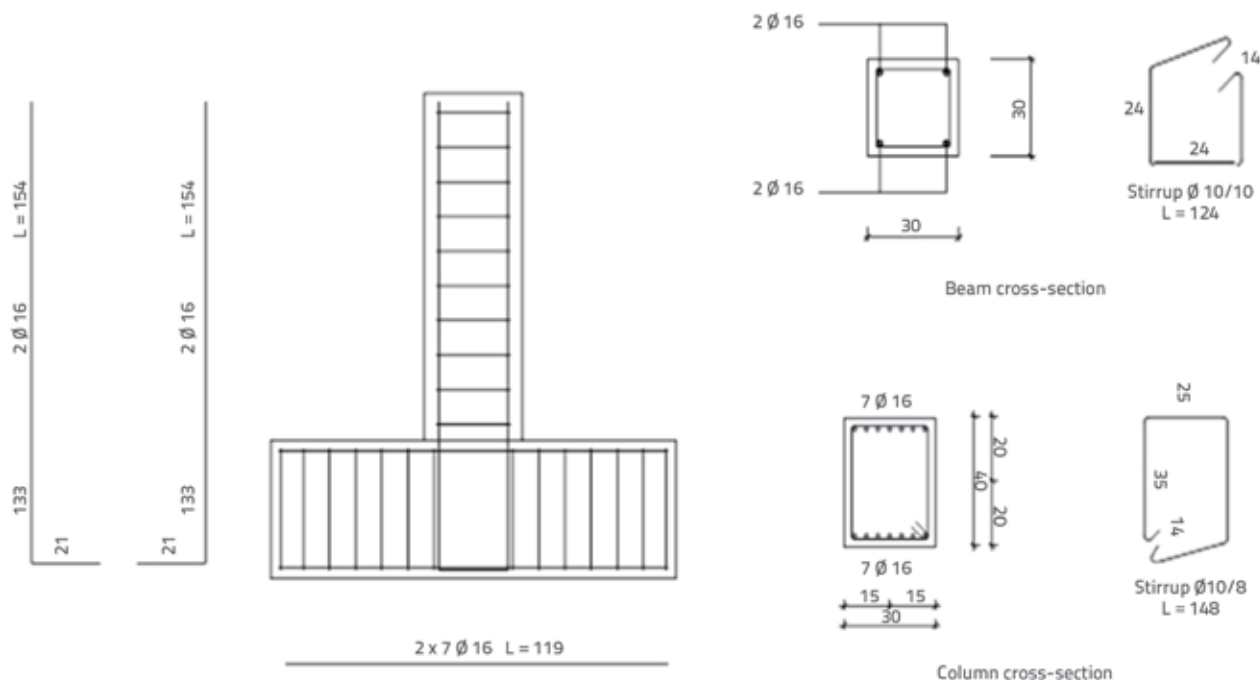


Figure 1. Details of test specimens

Table 1. Characteristics of concrete mixtures

Concrete types	Cement [kg/m <sup>3</sup> ]	Fly ash [kg/m <sup>3</sup> ]	Water [kg/m <sup>3</sup> ]	Water / (cement + fly ash)	Superplasticizer [kg/m <sup>3</sup> ]	Steel fibre [kg/m <sup>3</sup> ]	Aggregate [kg/m <sup>3</sup> ]
NCO	400	0	192	0.48	8	0	1870
NCO.5	400	0	192	0.48	8	39.3	1845
NC1	400	0	192	0.48	8	78.5	1820
SCCO	400	180	191	0.33	10.4	0	1600
SCCO.5	400	180	191	0.33	10.4	39.3	1550
SCC1	400	180	191	0.33	10.4	78.5	1510

area in order to investigate the crack-limiting feature of steel fibres. The results obtained by experimental testing of NC and SCC specimens were compared in terms of damage and energy dissipation capacities exhibited during the tests.

### 3. Materials

Table 1 shows characteristics of concrete mixtures used for six different mix designs. Portland type CEM I 42,5R cement according to the TS EN 197-1 [21] criteria, and basalt aggregates with a maximum aggregate size of 16 mm were used for all test specimens. Research aimed that the 28-day characteristic cylinder compressive strengths of the concrete test prototypes which are cast and wet-cured in the laboratory should not be less than 30 MPa. 150 mm cube and 150x300 mm cylinder concrete specimens were cast at the same time with the beam-column test specimens.

Laboratory test results of prototypes according to the TS EN 12390-3 [22] criteria showed that an average compressive strength of concrete cube specimens was 40 MPa. Furthermore, an average elastic modulus of concrete specimens was 35 GPa.

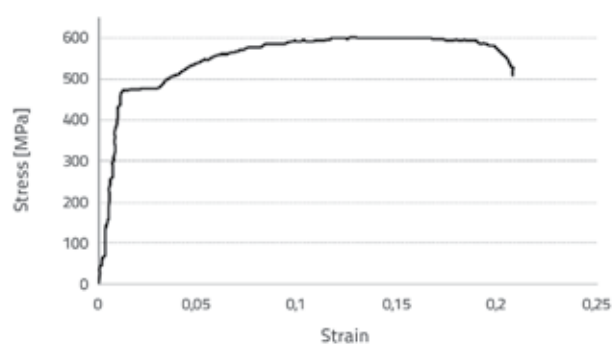


Figure 2. Stress-strain behaviour of steel

S420 steel reinforcement with a characteristic yield strength of 420 MPa was used. Mechanical properties of steel rebars and characterization test results according to the TS EN ISO 6892-1 [23] are shown in Figure 2 and Table 2. For the fibre-concrete mixture, steel fibres with the yield strength of 1100 MPa, 50 mm in length and 1 mm in diameter, were added at

0.5 % and 1 % volume fractions of concrete. A superplasticizer according to TS EN 934-2 [24] was used in the self-compacting concrete mixture to increase workability of the mixtures. Class F fly ash from Afsin-Elbistan Thermal Power Plant was used. The fly ash-cement ratio was 0.45 for self-compacting concrete, while water to cement plus fly ash ratio was 0.33 for all specimens.

Table 2. Characteristics of steel rebars

Rebar	Yield strength [MPa]	Tensile strength [MPa]	Elongation [%]	Elastic modulus [GPa]
S420	477	600	21.1	200

### 4. Experimental program and testing procedure

A total of six full-scale concrete beam-column specimens were tested in the Structures Laboratory of Civil Engineering Faculty of Harran University. In all test specimens, columns were positioned horizontally, and beams vertically (Figure 3). The load was applied to the top end of the beam using a hydraulic actuator mounted on the reaction wall. Besides, a constant load was applied to the column with a hydraulic jack in the horizontal position. The two ends of the column were fixed so that they did not displace horizontally and vertically. Only rotation was permitted.

The beam column joints subjected to reverse cyclic loading were tested by displacement control loading. The displacement-controlled loading, involving three equal displacement cycles applied to the top of the beam for each loading step, is shown in Figure 4. For all specimens, the drift ratio started from 0.75 % to a maximum of 5 %. Target displacements determined for displacement-controlled loading were calculated by multiplying the drift ratio with the distance between the point where the load was applied and the axis passing through the centre of the column. The displacement of the beam end and the load applied to the top of the beam were observed using the computer data-collection application attached to the tester. As a result of the experiments, the data acquisition system produced appropriate load drift ratio graphs.

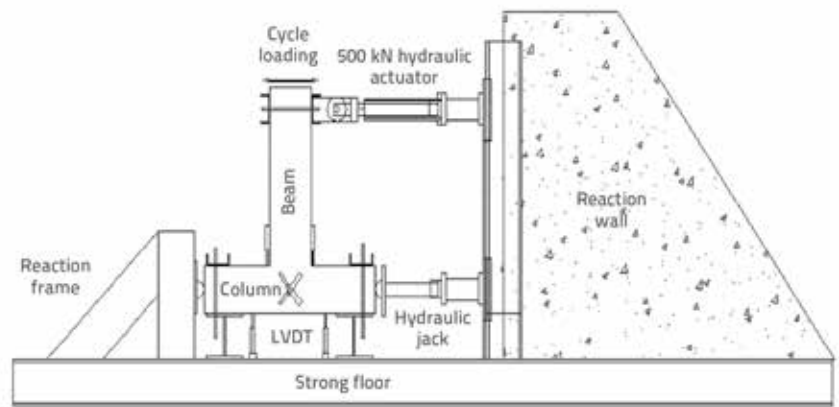


Figure 3. View of test setup

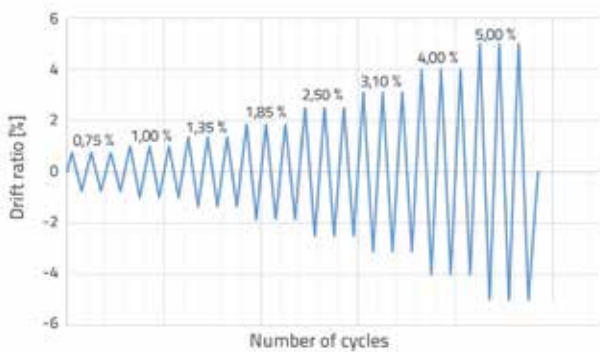


Figure 4. Displacement Controlled Loading

## 5. Test results and discussion

### 5.1. Failure modes

Figure 5 shows failure modes of six different specimens experimentally analysed under the cyclic load applied at the end of the beam. Formation of load-generated cracks on test specimens was evaluated as shown in Figure 6. For the beam-column specimens prepared using normal concrete and self-compacting concrete, flexural cracks parallel to the column surface formed in the beam at 1% drift ratio (Cracks 1). In the case of drift ratio of 2.5%, shear cracks began to appear in the joint region of these control specimens (Cracks 2). As the load application continued, the shear cracks expanded, and new shear cracks formed towards the top of the beam (Cracks 3). At the drift ratio of 3.1%, the concrete between the cracks 1 and 2 began to spall. When the loading continued, and the drift ratio reached 5%, cracks 3 expanded and concrete crushed. For fibre reinforced specimens (NC0.5, NC1, SCC0.5, and SCC1), flexural cracks formed at the drift ratio of 1.35% (Cracks 4). It is known that the addition of steel fibre increases shear strength of the reinforced concrete beam-column joints [25-26]. Likewise, when investigating the test results, it can be seen that the steel fibre reinforcement increases shear strength of specimens and, as a result of this, shear cracks do not form in the joint regions. During an earthquake, the beam-column joint region will not crush thus preventing human injuries. Preventing the loss of life can be considered the most fundamental benefit of using fibre reinforced concrete.



Figure 5. Failure modes of concrete specimens: a) Specimen NC0; b) Specimen NC0.5; c) Specimen NC1; d) Specimen SCC0; e) Specimen SCC0.5; f) Specimen SCC1

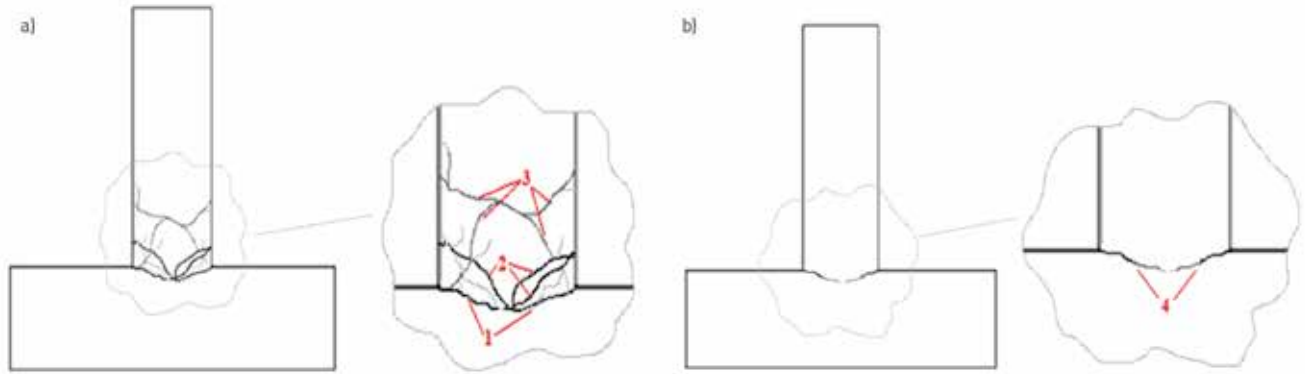


Figure 6. Cracks of specimens: a) without fibre; b) with fibre

## 5.2. Energy dissipation

The load-displacement hysteresis loops due to the reversed cyclic loading applied to the upper end of the beam at each

displacement-controlled loading step are shown in Figure 7. The total energy dissipation of every specimen at the beam-column joint was the sum of the area under the envelope curves of the load-displacement hysteresis loop.

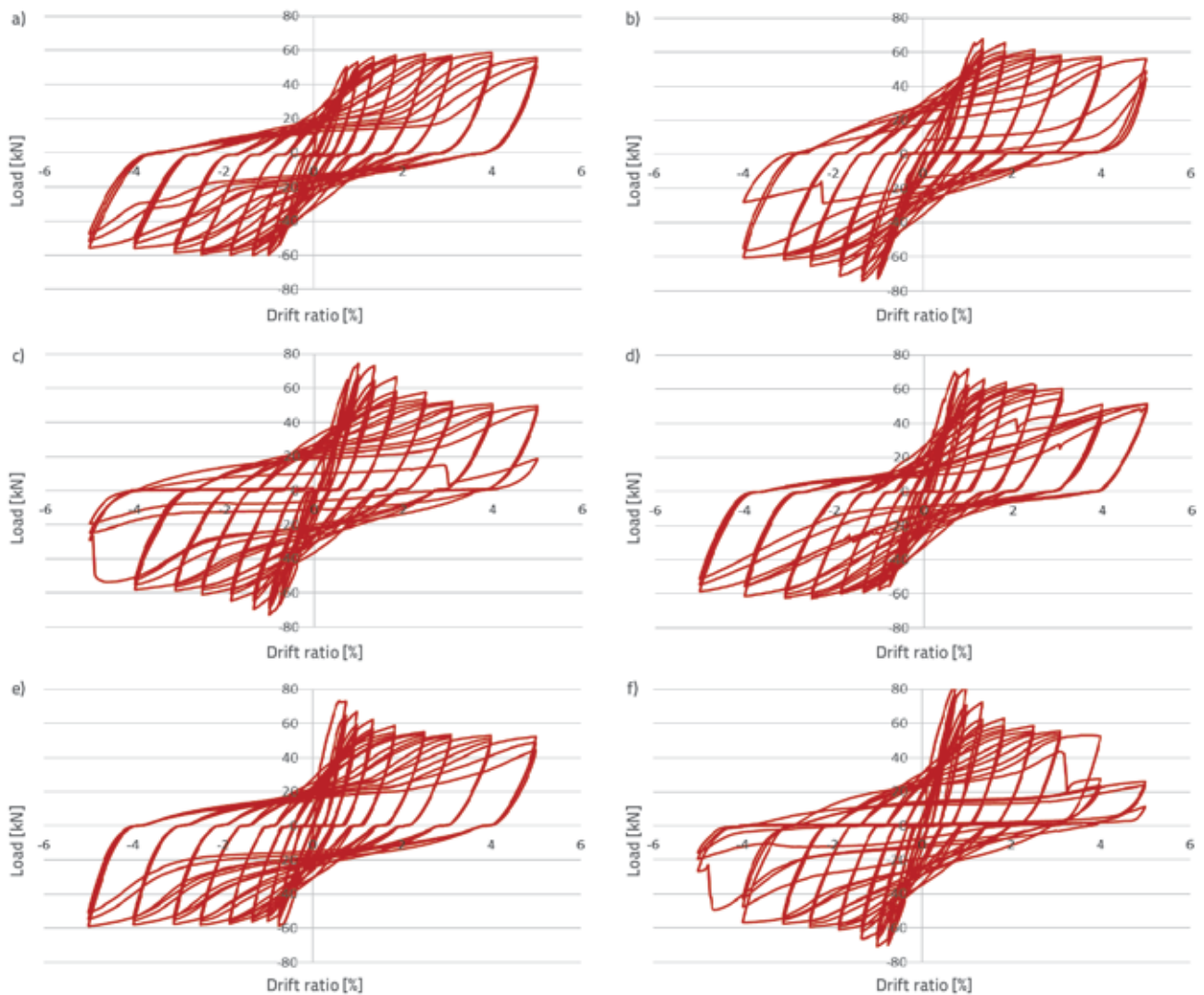


Figure 7. Specimens' load-drift ratio relationships: a) Specimen NC0; b) Specimen NC0.5; c) Specimen NC1; d) Specimen SCC0; e) Specimen SCC0.5; f) Specimen SCC1

Table 3. Ultimate load and energy dissipation capacities

Specimens name	Ultimate load [kN]	Maximum drift ratio [%]	Energy dissipation capacity [kNmm]	Increase of energy dissipation capacity [%]
NCO	58.7	5	8260	0.0
NC0.5	64.3	5	8300	0.5
NC1	75.3	5	9270	12
SCCO	66.2	5	8200	0.0
SCCO.5	66.2	5	8290	1.0
SCC1	79.2	5	9000	10

The ultimate load and energy dissipation capacities of all specimens are shown in Table 3. It can be seen in Table 3. that, for normal concrete, the ultimate load is 58.73 kN for the control specimen, it is 9 % greater for the specimen with 0.5 % fibre (NC0.5), while the increase amounts to 28 % for the specimen with 1 % fibre (NC1). While the energy dissipation capacity in normal concrete is 8260 kNmm, the increase is small enough to be neglected for specimen NC0.5, and it is by 12 % greater for specimen NC1. Similarly, for self-compacting concrete, the ultimate load for the control specimen is 66.17 kN. The increase is very small for 0.5 % fibre (SCCO.5), while the increase amounts to 20 % for a 1 % fibre (SCC1).

The energy dissipation capacity of the self-compacting concrete is 8200 and 8290 kNmm for the control specimen and specimen SCC0.5, respectively. The specimen with 1 % of steel fibre (SCC1) has dissipated the highest amount of energy, which is 9000 kNmm, i.e., the dissipation is greater by 10 % compared to the control specimen. There was no significant difference between the ultimate load and cumulative energy dissipation in NC and SCC specimens compared to their equivalent (i.e., the dissipated energy values of NC0.5 and SCC0.5 are pretty much same). This result shows that both concrete types could be used for similar purposes. Self-compacting concrete does not require compaction and is, therefore, superior to normal concrete regarding cost and labour.

### 5.3. Comparison of experimental test and finite element analysis results for NCO test specimens

In this section, the load-drift ratio hysteresis loops of the normal concrete control specimens are compared with the finite element analysis results. For the analysis

of the structure, a nonlinear finite element model was created in Abaqus/CAE [27]. The modelling was done using the C3D8R (an 8-node linear brick) finite element type, and the maximum mesh element size was taken to be 50 mm, which we consider to be an adequate approach, considering performance of computers available for this analysis. The concrete damage plasticity model was chosen as the concrete type, and two-dimensional "Truss" element was chosen as the reinforcement type. Also, steel bars were modelled as embedded reinforcement. A NCO concrete specimen from the finite element analysis is shown in Figure 8.

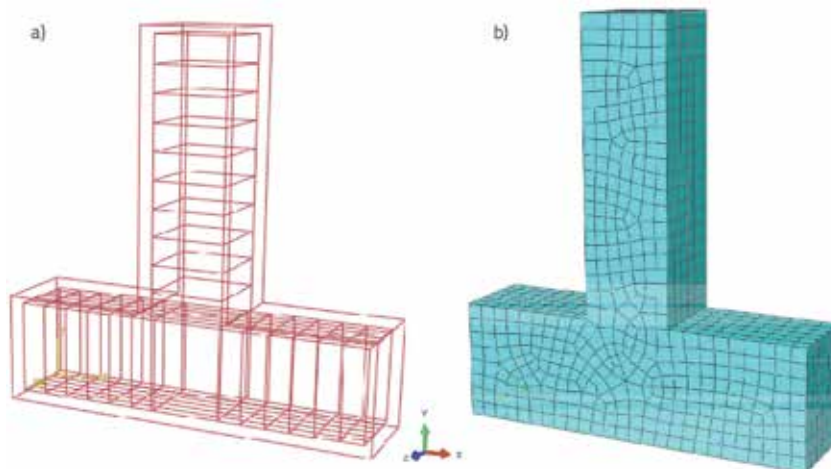


Figure 8. Finite element model: a) details of test specimens; b) mesh system

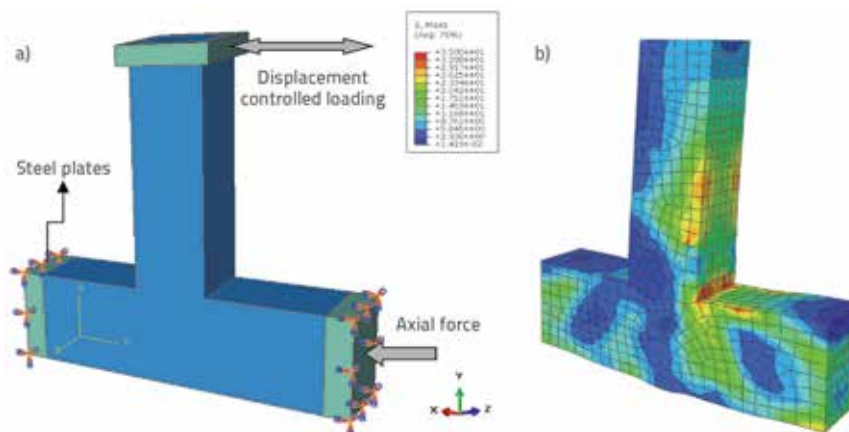


Figure 9. a) Boundary conditions of test specimens; b) stresses in FEM

The analysis was conducted by considering the same boundary conditions as in the experimental test setup. The displacement-controlled loading was applied to the top of the beam and the stresses occurring in critical regions were observed, as shown in Figure 9. The experimental test results obtained on specimen NCO, which was the reference model, were compared with the finite element method results. The load-drift ratio hysteresis loops of experimental and analytical test results are shown in Figure 10.

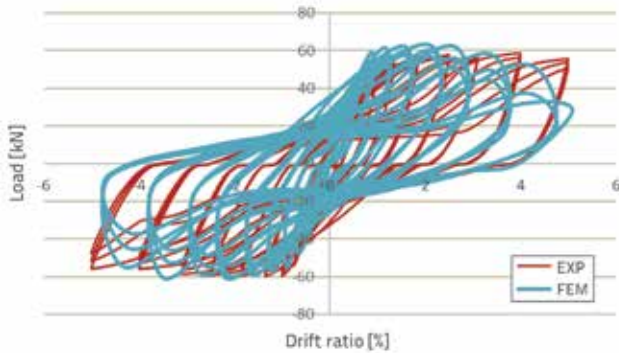


Figure 10. Comparison of experimental and finite element analysis results

The energy dissipation capacities and ultimate loads calculated from the experimental test and finite element analysis results of the control specimen are given in Table 4. A slight difference of 5.4% was established in the evaluation of energy dissipation capacity results. A good correspondence of results was established by comparison of the experimental test results and finite element analysis results. This result points to sufficient accuracy of the test set-up, the measurements and the preparation of specimens.

Table 4. Experimental test and finite element analysis results for specimen NCO.

Specimen NCO	Ultimate load [kN]	Maximum drift ratio [%]	Energy dissipation capacity [kNmm]
Experimental	58,73	5	8260
Finite element	62,75	5	8705

## 5.4. Rotation components

The drift ratio measured at the beam end consists of four main factors, as shown in Figure 11. These factors are: rotation of the plastic hinge region (a), regional rotations that occur due to large deformations of beam reinforcement at the joint (b), column rotation (c), and beam-column joint distortion (d). LVDTs were placed at appropriate positions on the beam-column joint to measure these components, which form the total rotation.

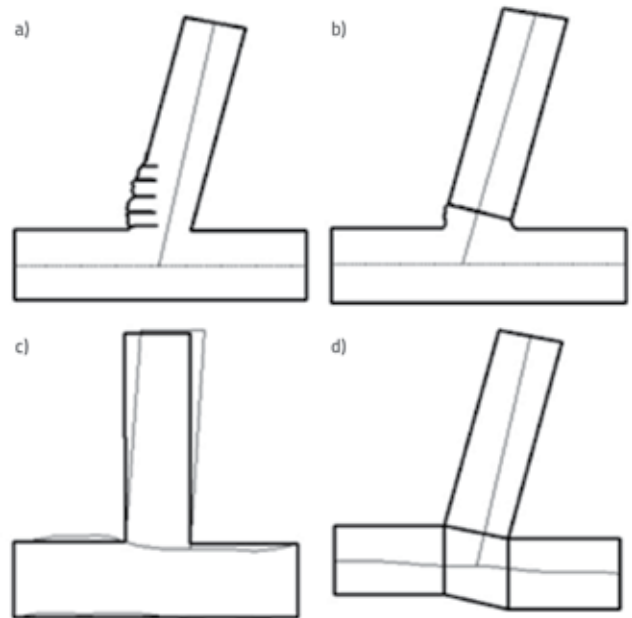


Figure 11. Total rotation factors: a) Plastic hinge; b) Strain of beam reinforcement at joint; c) Column rotation; d) Joint distortion

Linear variable differential transducers (LVDTs) were installed to measure the displacement and rotation at the end of the beam and at the beam-column joint. The calculation of total rotation from these three components is shown in Figure 12.

LVDTs 1 and 4, shown in Figure 13a, were placed in order to measure beam rotation. Elongations measured by LVDTs 1 and 4 after the start of the load are shown as  $l'_1$  and  $l'_4$ . The angle



Figure 12. Application of LVDTs: a) Column rotations; b) Beam rotations; c) Joint distortion

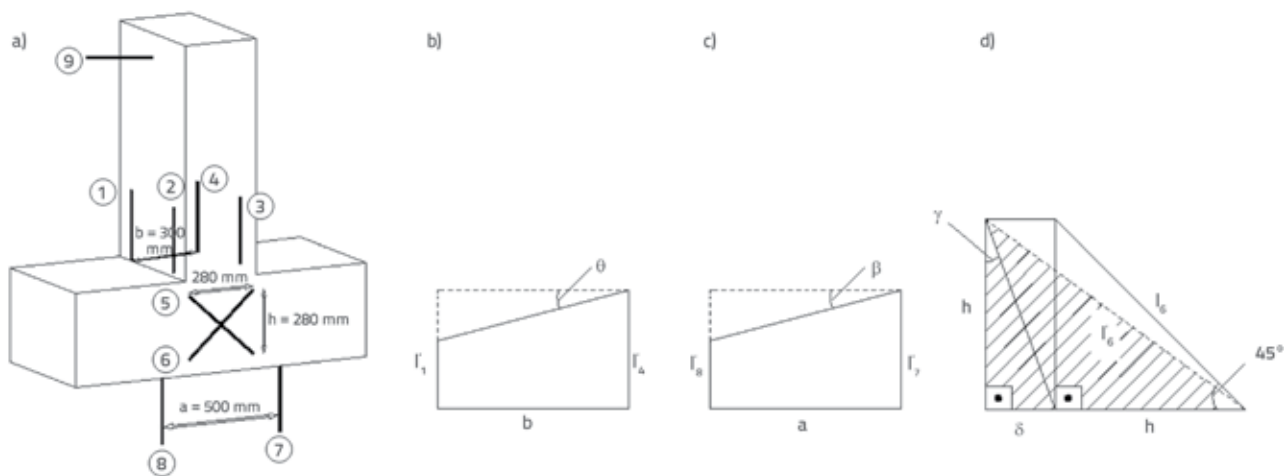


Figure 13. Joint rotation measurements a) Plan of LVDTs, b) Beam rotation, c) Column rotation, d) Joint distortion

$\theta$ , which expresses the beam rotation, was determined using geometric relations given in Figure 13b.

$$\delta = \frac{1}{2h} \left[ (l'_6)^2 \left\{ 1 - 2 \frac{h^2}{(l'_6)^2} \right\} \right] \quad (6)$$

$$tg\theta \approx \theta = \frac{l'_4 - l'_5}{b} \quad (1) \quad \delta = tg\gamma \approx \gamma = \frac{1}{2h^2} \left[ (l'_6)^2 \left\{ 1 - 2 \frac{h^2}{(l'_6)^2} \right\} \right] \quad (7)$$

LVDTs 7 and 8 were placed in order to calculate column rotation. Elongations measured by LVDT 7 and 8 after the start of the test are marked as  $l'_7$  and  $l'_8$ . Using geometrical relations shown in Figure 13c:

$$tg\beta \approx \beta = \frac{l'_7 - l'_8}{a} \quad (2)$$

the angle  $\beta$ , which indicates column rotation, was calculated.

As shown in Figure 13a, LVDTs 5 and 6 were placed on the test specimen. The horizontal distance between LVDTs, measured length, and horizontal component of LVDT 6 after the start of the experiment, are designated as  $h$ ,  $l'_6$ ,  $\delta+h$ , respectively.

The angle  $\gamma$ , showing joint distortion, is calculated based on Figure 13d and the following geometric relationships:

$$h^2 + (\delta + h)^2 = (l'_6)^2 \quad (3)$$

$$h^2 + \delta^2 + 2\delta h + h^2 = (l'_6)^2 \quad (4)$$

$$\frac{2h^2}{(l'_6)^2} + \frac{\delta^2}{(l'_6)^2} + \frac{2\delta h}{(l'_6)^2} = 1, \quad (5)$$

$$\frac{\delta^2}{(l'_6)^2} \text{ (neglected)}$$

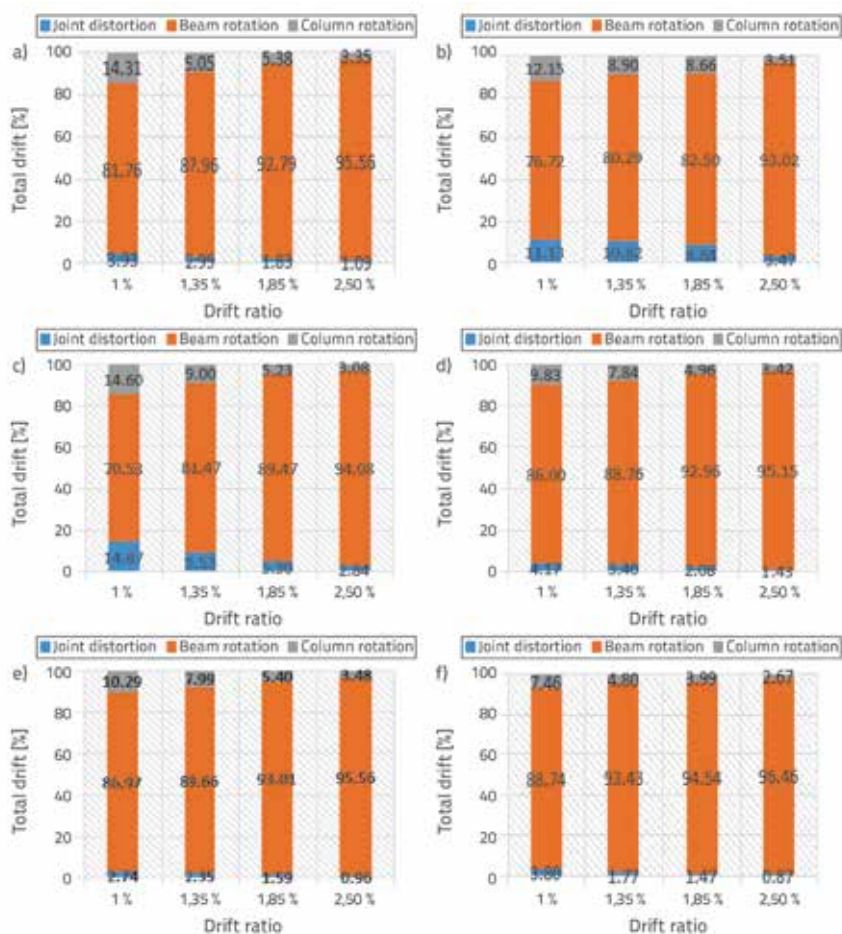


Figure 14. Percentage of rotation due to each component in total rotations: a) Specimen NCO; b) Specimen NCO.5; c) Specimen NC1; d) Specimen SCC0; e) Specimen SCC0.5; f) Specimen SCC1

The total rotation of the joint was determined as the sum of the factors constituting the rotation. The total dissipated energy at the beam-column joint is shared as the ratio of each component rotation to the total rotation. As the drift ratio increases from 0.75 % to 5 %, rotations increase at the joint, the joint weakens, and a plastic hinge forms on the beam section near the column face. For this reason, 1-2.5 % of the drift was taken into consideration when evaluating distribution rates for the factors of the total dissipated energy. The strain of beam reinforcement at the joint was neglected since the rotation is small compared to other components. Three components of total energy were taken into account, as shown in Figure 14.

It is clear that beam rotation is responsible for a major part of the energy dissipated at the joint. This situation shows that the joint was designed according to the strong column-weak beam concept. For small drift ratios such as 1 %, the dissipated energy due to column rotation and joint distortion is high, but there are no large cracks at the joint. As the drift ratio increases from 1 % to 2.5 %, the energy dissipation due to column rotation and joint distortion decreases, and the dissipated energy caused by beam rotation is more prominent. In the drift ratio range investigated in this study, the increases of steel fibre rate do not affect the dissipated energy rates, as no large cracks were formed at the beam-column joint.

## 6. Conclusions

Concrete beam-column joint assemblies, reinforced with varying amounts of steel fibres and subjected to displacement controlled reversed cyclic loading, were tested in this study. Steel fibres in the proportion of 0, 0.5 and 1.0 % by volume

were added to the Normal Concrete (NC) and Self-Compacting Concrete (SCC) specimens. Based on the study and analysis of experimental results, the following conclusions can be drawn: The strength capacity and ductility could be enhanced by using fibres in the joint of the beam and column. Approximately 90 % of the total energy of the beam-column joint was dissipated as a result of beam rotation.

The dissipated energy due to column rotation and joint distortion was quite small compared to the energy dissipated due to beam rotation. While there is no increase in energy dissipation capacity compared to the control specimen for the 0.5 % steel fibre ratio, a significant increase (10-12 %) in energy dissipation capacity occurs for the 1 % steel fibre ratio. This increase is very essential for earthquake resistant design of reinforced concrete structures.

As a result of shear strength increase in the fibre reinforced specimen, the plastic hinge region becomes smaller, and the damage to concrete is limited. The concrete beam-column joints with fibre reinforcement will reduce human injuries during earthquakes.

NC and SCC have similar behaviour with respect to their energy dissipation capacity. They can be used interchangeably in building construction. However, SCC is more cost-effective than normal concrete as it does not need mechanical vibration and labour for the compaction process.

## Acknowledgments

This research was supported by Harran University Scientific Research Projects Coordination Unit of Turkey (HUBAK project numbers: 16073 and 17122)

## REFERENCES

- [1] Kumar, V., Shamim, M.: Influence of Beam Reinforcement on Exterior Beam-Column Joints, *Journal of Structural Engineering*, 26 (1999) 2, pp. 123-127.
- [2] Choi, H.K., Choi, Y.C., Choi, C.S.: Development and testing of precast concrete beam-to-column connections, *Engineering Structures*, 56 (2013), pp. 1820-1835.
- [3] Rajagopal, S., Prabavathy, S.: Study of exterior beam-column joint with different joint core and anchorage details under reversal loading, *Structural Engineering and Mechanics*, 46 (2013) 6, pp.809-825.
- [4] Yuksel, E., Karadogan, H.F., Bal, İ.E.: Seismic behaviour of two exterior beam-column connections made of normal-strength concrete developed for precast construction. *Engineering Structures*, 99 (2015), pp.157-172.
- [5] Isik, E., Isik, M.F., Bulbul, M.A.: Web based evaluation of earthquake damages for reinforced concrete buildings, *Earthquakes and Structures*, 13 (2017), pp. 387-396.
- [6] Das, P., Choudhury, S.: Experimental Study on Fibre-Reinforced Concrete Beam-Column Joint with Ductile Detailing Under Reverse Cyclic Loading, *International Journal of Engineering & Technology*, 7 (2018) 3.4, pp. 85-89.
- [7] Sharbatdar, M.K., Saatcioglu, M., Benmokrane, B., El-Salakawy, E.: Behaviour of FRP reinforced concrete beam-column joints under cyclic loading, 3<sup>rd</sup> Int. Conf. on Durability & Field Applications of Fibre Reinforced Polymer (FRP) Composites for Construction, (CDCC-07), Univ. of Sherbrook, Canada, 2007.
- [8] Hasaballa, M.H.: Seismic Behaviour of Exterior GFRP Reinforced Concrete Beam-Column Joints, M.Sc. Thesis, University of Manitoba, Manitoba, Canada, 2009.
- [9] Mady, M., Elragaby, A., Elsalakawy, E.: Seismic behaviour of beam-column joints reinforced with GFRP bars and stirrups, *Journal of Composites for Construction*, 15 (2011) 6, pp. 875-886.
- [10] Tavakoli, H.R., Jalali, P., Mahmoudi, S.: Experimental evaluation of the effects of adding steel fibre on the post-cyclic behaviour of reinforced self-compacting concrete beams. *Journal of Building Engineering*, 32 (2020), 101673. 2019,25:100771.
- [11] Siddika A., et al.: Strengthening of reinforced concrete beams by using fibre-reinforced polymer composites: A review, *Journal of Building Engineering*, 25 (2019), pp. 100798.
- [12] Oh, B.H.: Flexural Analysis of Reinforced Concrete Beams Containing Steel Fibres, *Journal of Structural Engineering*, 118 (1992) 10.

- [13] Parra-Montesinos, G.J., Wight, J.K.: Seismic Response of Exterior RC Column-to-Steel Beam Connections, *Journal of Structural Engineering*, ASCE, 126 (2000) 10, pp. 1113-1121.
- [14] Jiuru, T., Chaobin, H., Kaijian, Y., Yongcheng, Y.: Seismic Behaviour and Shear Strength of Framed Joint Using Steel-Fibre Reinforced Concrete, *Journal of Structural Engineering*, ASCE, 118 (1992) 2, pp. 341-358.
- [15] Caballero, K.E., Bonet, J.L., Avarro, J.N., Marti, J.R.: Behaviour of Steel-Fibre-Reinforced Normal-Strength Concrete Slender Columns under Cyclic Loading, *Engineering Structures*, 39 (2012), pp. 162-175.
- [16] Bedirhanoğlu, İ., İlki, A.: HPRCC for retrofitting of reinforced concrete members built with low strength concrete, *ITU Journal Series D: Engineering*, 8 (2009) 6, pp. 146-156.
- [17] Yurdakul, Ö., Avşar, Ö.: Structural repairing of damaged reinforced concrete beam-column assemblies with CFRPs, *Structural Engineering and Mechanics*, 54 (2015) 3, pp. 521-43.
- [18] Hamad, B.S., Haider, E.Y.A.: Effect of Steel Fibres on Bond Strength of Hooked Bars in High-Strength Concrete", *Journal of Materials in Civil Engineering*, 23 (2011) 5, pp. 673-681.
- [19] Gencoğlu, M., Eren, I.: An experimental study on the effect of steel fibre reinforced concrete on the behaviour of the exterior beam-column joints subjected to reversal cyclic loading, *Turk J Eng Environ Sci*, 26 (2002), pp. 493-502.
- [20] Turkish Standardization Institute, Requirements for design and construction of reinforced concrete structures TS 500, Ankara, Turkey, 2000.
- [21] TSI, TS EN 197-1: Cement-part 1: Composition, specification and conformity criteria for common cements, Ankara, Turkey: Turkish Standard Institute, 2012.
- [22] TS EN 12390-3. Testing hardened concrete - Part 3: Compressive strength of test specimens, Ankara, Turkey: Turkish Standard Institute, 2019.
- [23] TS EN ISO 6892-1 Metallic materials - Tensile testing - Part 1: Method of test at room temperature, Ankara, Turkey: Turkish Standard Institute, 2020.
- [24] TS EN 934-2+A1: Admixtures for concrete, mortar and grout-Part 2: concrete admixtures-definitions, requirements, conformity, marking and labelling. Ankara, Turkey: Turkish Standard Institute, 2013.
- [25] Junior, A.L.M., Vedoato, A.P.: The Shear Strength of Steel Fibre-Reinforced Concrete Beams, *IBRACON Structures and Materials Journal*, Sao Paulo, 4 (2011) 5.
- [26] Cucchiara, C., Fossetti, M., Papia, M.: Steel fibre and transverse reinforcement effects on the behaviour of high strength concrete beams, *Structural Engineering and Mechanics*, 42 (2012) 4, pp. 551-570.
- [27] Abaqus: ABAQUS user's manual version 6.14-1, Hibbit, Karlsson & Sorensen, Inc., Providence, RI, USA, 2014.